Preparation and Characterization of Polyoxometalate/Protein Ultrathin Films Grown on Electrode Surfaces Using Layer-by-Layer Assembly

Kai Jiang, Hongxia Zhang, Curtis Shannon,* and Wei Zhan*

Department of Chemistry and Biochemistry, Auburn University, Auburn, Alabama 36849

Received December 23, 2007

We report a new electrostatic layer-by-layer assembly method for the controlled deposition of electrocatalytically active enzymes onto electrode surfaces using polyoxometalate as the counteranion. Cytochrome *c* (*cyt c*), a redox active protein, and $P_2W_{18}O_{62}^{6-}$, a Dawson-type polyoxometalate, were deposited onto glassy carbon electrodes by two procedures: static dipping and electrochemical cycling. Cyclic voltammetry and UV−vis spectroscopy reveal that approximately 1.5×10^{-10} mol/cm^2 of $P_2W_{18}O_{62}^{6-}$ and 2.2×10^{-11} mol/cm^2 of cytochrome c are deposited per cycle, which correspond to approximately one monolayer of each molecule. The thicknesses of the resulting films measured by atomic force microscopy also indicate that the films are formed in a layer-by-layer fashion. Experimental factors that affect electron-transfer rate in these films, such as scan rate and film thickness, were systematically analyzed. The use of $\{P_2W_{18}O_{62}^{6-}/cyt\ c\}_n$ films to catalyze hydrogen peroxide reduction was demonstrated.

Introduction

In addition to yielding fundamental insights into biological electron-transfer processes, the use of redox enzymes to interface with external solid electrodes has many potential applications, such as amperometric biosensors and biofuel cells.[1−7] Over the past years, a wide variety of experimental strategies[8−10] have been investigated to establish reliable electrical communication between enzymes and electrodes, including layer-by-layer (LbL) deposition, the direct modification of enzymes with electron relays, and the reconstitution of apo-flavoenzymes (i.e., glucose oxidase) on self-assembled monolayers.

The immobilization of redox proteins such as cytochrome *c* (*cyt c*) onto electrode surfaces through LbL deposition has been highly successful in practice.[11−19] Because of their multiple charges and flexible backbones, polyelectrolytes are often the material of choice in forming LbL thin films. While the multiple charges collectively enforce strong binding between the polymer molecule and the oppositely charged surface, the flexible polymer chain can easily adjust to the local surface structure and charge distribution. Nevertheless, several LbL film preparation schemes exist where metal and inorganic nanoparticles are used instead of polyelectrolytes. For example, He et al. demonstrated a LbL formation of hemoglobin multilayer film using 35 nm SiO_2 nanoparticles.[20] Polyoxometalates (POMs), a large family of charged, nanoscopic inorganic clusters, are attractive materials for electrode modification because of their reversible redox behavior, good chemical stability, and electronic conductivity.[21−29] We expect POMs to be excellent counterions for LbL deposition because of their relatively high surface charge and their versatile self-assembly capabilities.[30] Compared to previously used nanoparticles, POMs are at least an order of magnitude smaller in size and should form more conformal films. Moreover, these inorganic nanoclusters themselves show electrocatalytic activity (e.g., for reduction of hydrogen peroxide,[26] nitrogen monoxide,[28] and iodate.[29]), a characteristic worth exploring in designing new LbL-based films.

Herein, we report on the preparation and characterization of LbL assembled ultrathin films containing model proteins and POMs. We show that stable, electrochemically well-behaved protein-containing films can be reproducibly prepared using nanoscopic (∼1 nm) POMs as the counterion. This approach departs from the majority of previously reported LbL procedures[31−34] in which polyelectrolyte counterions are generally employed. Cyclic voltammetry, UV−vis spectroscopy, and

* Corresponding authors: E-mail: wzz0001@auburn.edu, Phone: 334-844-6984, Fax: 334-844-6959. E-mail: shanncg@auburn.edu, Phone: 334-844-6964, Fax: 334-844-6959.

(1) Armstrong, F. A.; Hill, H. A. O.; Walton, N. J. *Q. Rev. Biophys.* **1985**, *18*, 261−322.
(2) Zhou, Y. L.; Hu, N. F.; Zeng, Y. H.; Rusling, J. F. *Langmuir* **2002**, *18*, 211−219.
(3) Shen, L.; Hu, N. F. *Biochim. Biophys. Acta* **2004**, *1608*, 23−33.
(4) Shan, W. J.; He, P. L.; Hu, N. F. *Electrochim. Acta* **2005**, *51*, 432−440.
(5) Sultana, N.; Schenkman, J. B.; Rusling, J. F. *J. Am. Chem. Soc.* **2005**, *127*, 13460−13461.
(6) Xu, J. M.; Li, W.; Yin, Q. F.; Zhu, Y. L. *Electrochim. Acta* **2007**, *52*, 3601−3606.
(7) Willner, I.; Katz, E. *Angew. Chem., Int. Ed.* **2000**, *39*, 1180−1218.
(8) Degani, Y.; Heller, A. *J. Am. Chem. Soc.* **1988**, *110*, 2615−2620.
(9) Willner, I.; Heleg-Shabtai, V.; Blonder, R.; Katz, E.; Tao, G. L.; Buckmann, A. F.; Heller, A. *J. Am. Chem. Soc.* **1996**, *118*, 10321−10322.
(10) Bernhardt, P. V. *Aust. J. Chem.* **2006**, *59*, 233−256.
(11) Lvov, Y.; Ariga, K.; Ichinose, I.; Kunitake, T. *J. Am. Chem. Soc.* **1995**, *117*, 6117−6123.
(12) Lvov, Y. M.; Lu, Z. Q.; Schenkman, J. B.; Zu, X. L.; Rusling, J. F. *J. Am. Chem. Soc.* **1998**, *120*, 4073−4080.
(13) Jin, Y. D.; Shao, Y.; Dong, S. J. *Langmuir* **2003**, *19*, 4771−4777.
(14) Lojou, E.; Bianco, P. *J. Electroanal. Chem.* **2003**, *557*, 37−47.
(15) Beissenhirtz, M. K.; Scheller, F. W.; Stocklein, W. F. M.; Kurth, D. G.; Mohwald, H.; Lisdat, F. *Angew. Chem., Int. Ed.* **2004**, *43*, 4357−4360.
(16) He, P. L.; Hu, N. F. *Electroanalysis* **2004**, *16*, 1122−1131.
(17) Lu, H. Y.; Hu, N. F. *Electroanalysis* **2006**, *18*, 1511−1522.
(18) Lojou, E.; Bianco, P. *Electroanalysis* **2006**, *18*, 2426−2434.
(19) Feng, J. J.; Xu, J. J.; Chen, H. Y. *Biosens. Bioelectron.* **2007**, *22*, 1618−1624.
(20) He, P. L.; Hu, N. F.; Rusling, J. F. *Langmuir* **2004**, *20*, 722−729.
(21) Ingersoll, D.; Kulesza, P. J.; Faulkner, L. R. *J. Electrochem. Soc.* **1994**, *141*, 140−147.
(22) Kuhn, A.; Anson, F. C. *Langmuir* **1996**, *12*, 5481−5488.
(23) Sadakane, M.; Steckhan, E. *Chem. Rev.* **1998**, *98*, 219−237.
(24) Katsoulis, D. E. *Chem. Rev.* **1998**, *98*, 359−387.
(25) Liu, J. Y.; Cheng, L.; Li, B. F.; Dong, S. J. *Langmuir* **2000**, *16*, 7471−7476.
(26) Martel, D.; Kuhn, A. *Electrochim. Acta* **2000**, *45*, 1829−1836.
(27) Wang, B. Q.; Cheng, L.; Dong, S. J. *J. Electroanal. Chem.* **2001**, *516*, 17−22.
(28) Liu, S. Q.; Volkmer, D.; Kurth, D. G. *Anal. Chem.* **2004**, *76*, 4579−4582.
(29) Lin, X. Q.; Jiang, C. M. *Anal. Sci.* **2006**, *22*, 697−700.
(30) Liu, T. B.; Diemann, E.; Li, H. L.; Dress, A. W. M.; Muller, A. *Nature* **2003**, *426*, 59−62.
(31) Decher, G. *Science* **1997**, *277*, 1232−1237.
(32) Rusling, J. F.; Forster, R. J. *J. Colloid Interface Sci.* **2003**, *262*, 1−15.
(33) Tang, Z. Y.; Wang, Y.; Podsiadlo, P.; Kotov, N. A. *Adv. Mater.* **2006**, *18*, 3203−3224.

10.1021/la704015j CCC: $40.75
Published on Web 02/20/2008

atomic force microscopy (AFM) are used to characterize films formed using *cyt c* and $P_2W_{18}O_{62}^{6-}$, a Dawson-type POM. The electron transfer of these films as a function of film thickness is systematically analyzed. Finally, the use of these films to catalyze hydrogen peroxide reduction is shown.

Experimental Section

Reagents. Cytochrome *c* (MW 12 300) and myoglobin (MW 16 900) from horse heart were obtained from Sigma. Tris(2,2′-bipyridyl)dichlororuthenium(II) hexahydrate ($Ru(bpy)_3Cl_2 \cdot 6H_2O$, 99.95%) was obtained from Aldrich. Hydrogen peroxide (H_2O_2, 30%), potassium dihydrogen phosphate (KH_2PO_4), dipotassium phosphate (K_2HPO_4), and potassium chloride (KCl) were purchased from Fisher Scientific. Phosphate buffer saline (PBS, 0.1 M at pH = 7.4) was prepared by dissolving suitable amounts of KH_2PO_4 and K_2HPO_4 in water. All solutions employed in these experiments were prepared using 18.2 MΩ·cm deionized water (Millipore). Polyoxometalates, including $K_6P_2W_{18}O_{62}$ and $K_{12}H_2P_2W_{12}O_{48}$, were synthesized following reported procedures.[35]

Film Assembly. Prior to film assembly, the glassy carbon electrode (Bioanalytical Systems, diameter = 3 mm) was polished with 1.0, 0.3, and 0.05 μm alumina slurries to a mirrorlike finish. The electrode was then sonicated in 1:1 (w/w) HNO_3/water solution, ethanol, and water, each step for 5 min, and polarized at 1.2 V (vs Ag/AgCl) for 5 min in 0.5 M NaOH aqueous solution with a Pt wire counter electrode. This treatment renders the electrode negatively charged. The electrode was then immersed in a 5 mg/mL $Ru(bpy)_3Cl_2 \cdot 6H_2O$ aqueous solution for 1 h, resulting a positively charged, $Ru(bpy)_3^{2+}$ layer on the surface. Finally, the positively charged electrode was immersed into corresponding POM (0.2 mM) and protein solutions (1 mg/mL) for 15 min for each adsorption step. Between each step, the modified electrode was rinsed with deionized water and dried in a stream of flowing nitrogen. The POM/$Ru(bpy)_3^{2+}$ layered films were prepared similarly except that the *cyt c* solution was replaced by a 5 mg/mL $Ru(bpy)_3Cl_2$ aqueous solution.[21] For consistency, all the films used in this study were terminated by a POM layer.

The ultrathin POM/protein LbL films can also be prepared under electrochemical conditions. Initially, the glassy carbon electrode was polished, rinsed, and polarized as described above. Then, it was subjected to potential scan between −0.8 and 0 V (vs Ag/AgCl) at 0.1 V/s for 400 cycles in 5 mg/mL $Ru(bpy)_3Cl_2$ aqueous solution. This $Ru(bpy)_3^{2+}$ modified electrode was then scanned in a POM solution (0.2 mM, 0.2−0.9 V vs Ag/AgCl) followed by in a *cyt c* solution (0.5 mg/mL in 0.05 M H_2SO_4, −0.55−0.05 V vs Ag/AgCl), each for 100 cycles.

Glass substrates (Corning 7409) for UV−vis measurements (0.6 × 2 cm^2, 1 mm thick) were sonicated in Micro-90 washing solution (International Products Co.) for 1 h and then in a cleaning solution (60% ethanol + 39% water + 1% NaOH, w/w) for 30 min at 50 °C and finally rinsed by water. Slides subjected to this treatment have a negatively charged surface. A positively charged $Ru(bpy)_3^{2+}$ monolayer was then formed on the glass surface by immersing the slides into $Ru(bpy)_3^{2+}$ solution for 1 h. The $\{P_2W_{18}O_{62}^{6-}/cyt\ c\}_n$ layers were assembled by immersing the slides into the corresponding solutions for 15 min.

UV−vis Spectroscopy. All measurements were carried out using a UV−visible spectrophotometer (Cary 50 Bio, Varian).

AFM Measurements. AFM measurements to determine film thickness were performed using protein/POM films formed on mica. To facilitate the LbL assembly process on these substrates, freshly cleaved mica specimens were first immersed in a 5 mg/mL $Ru(bpy)_3Cl_2$ aqueous solution overnight to accumulate positive charges on surface. After thoroughly rinsing the mica samples with DI water, POM/protein films were assembled using the same static dipping procedure we used for glassy carbon electrodes. Patterning

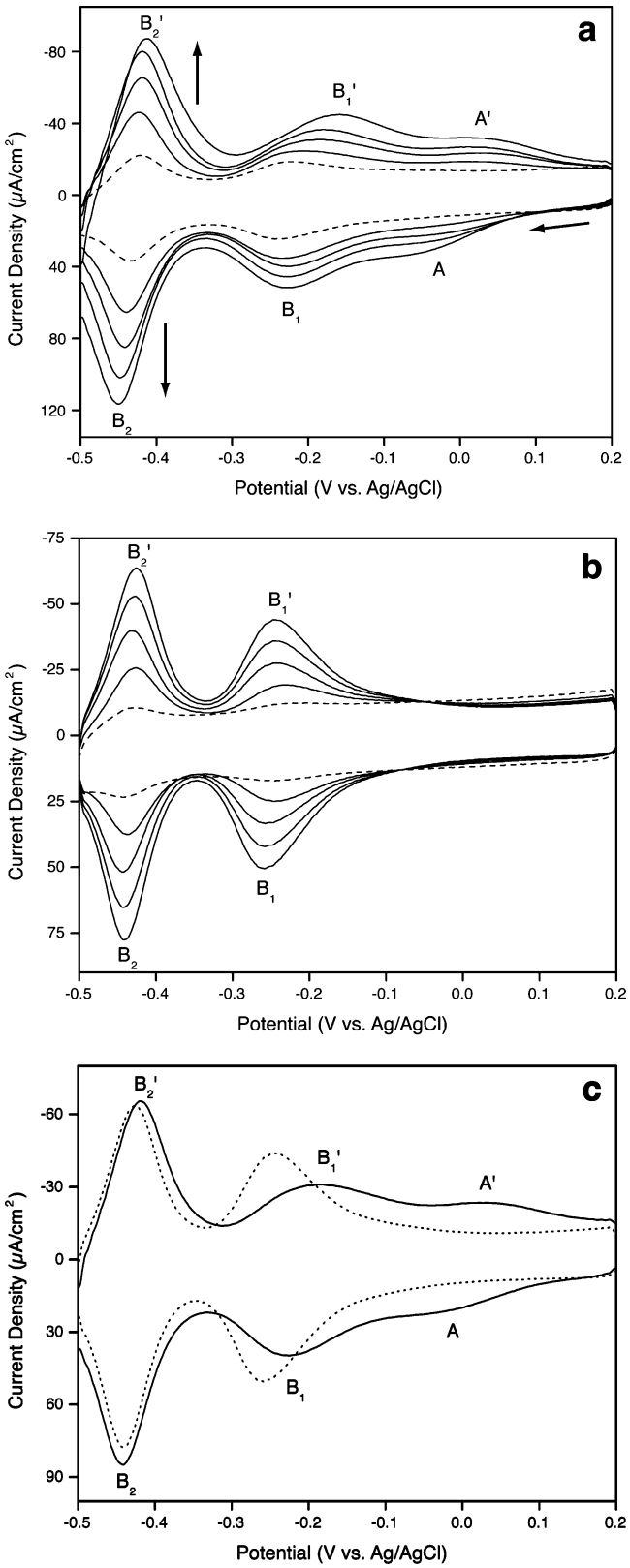

Figure 1. Layer-by-layer formation of $P_2W_{18}O_{62}^{6-}$ and *cyt c* (or $Ru(bpy)_3^{2+}$) thin films characterized by cyclic voltammetry (CV). The multilayered films were formed by alternately dipping a glassy carbon electrode (GCE) in respective POM and protein (or $Ru(bpy)_3^{2+}$) solutions. The first layer (dashed line) of $P_2W_{18}O_{62}^{6-}$ was electrostatically attracted onto the electrode surface by a preadsorbed $Ru(bpy)_3^{2+}$ layer. Supporting electrolyte, 0.1 M H_2SO_4 aqueous solution; scan rate, 0.1 V/s. (a) $\{P_2W_{18}O_{62}^{6-}/cyt\ c\}_n$, $n = 1-4$; (b) $\{P_2W_{18}O_{62}^{6-}/Ru(bpy)_3^{2+}\}_n$, $n = 1-4$; (c) comparison of $\{P_2W_{18}O_{62}^{6-}/cyt\ c\}_2$ and $\{P_2W_{18}O_{62}^{6-}/Ru(bpy)_3^{2+}\}_4$ (dotted line).

(34) Ariga, K.; Nakanishi, T.; Michinobu, T. *J. Nanosci. Nanotechnol.* **2006**, *6*, 2278−2301.

(35) Ginsberg, A. P. *Inorganic Syntheses*; Wiley-Interscience: New York, 1990; Vol. 27.

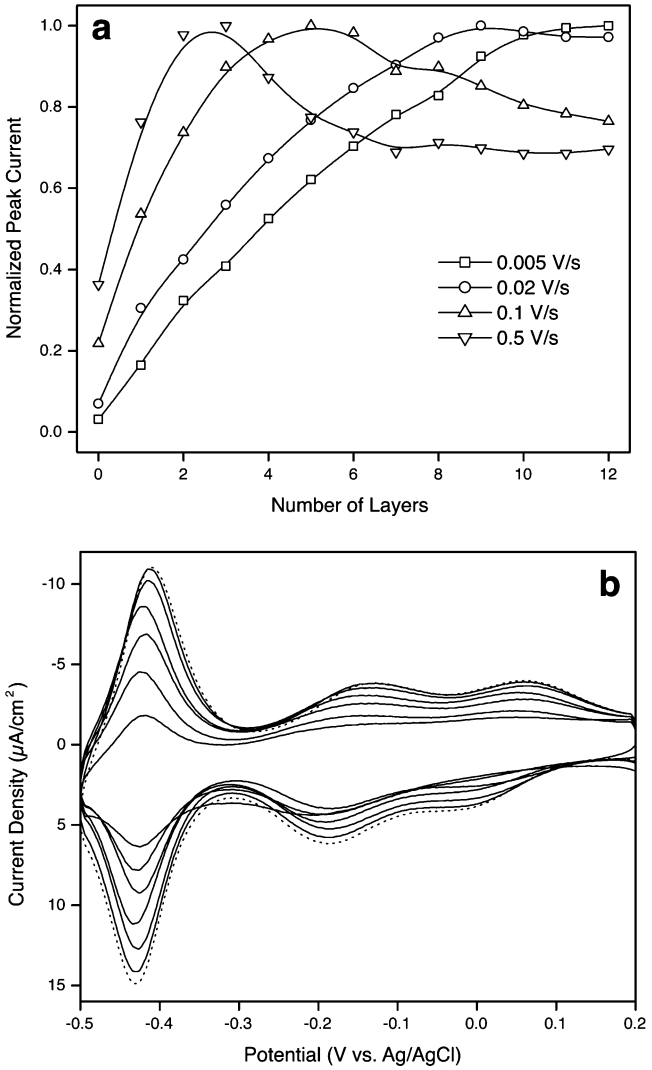

Figure 2. Electrochemical responses of a $\{P_2W_{18}O_{62}^{6-}/cyt\ c\}_n$ film under different CV scan rate. (a) Normalized peak (B_2' as in Figure 1a) current of $\{P_2W_{18}O_{62}^{6-}/cyt\ c\}_n$ ($n = 1-12$) at different scan rate. (b) Cyclic voltammograms of $\{P_2W_{18}O_{62}^{6-}/cyt\ c\}_n$ at 0.005 V/s (solid line, $n = 1$, 3, 5, 7, 9, and11; doted line, $n = 12$).

of LbL films on mica substrates was realized by a lift-off process following a lithography-based micropatterning procedure[36] reported previously.

All AFM experiments were performed using a Park Scientific Instruments Autoprobe CP scanning probe microscope in tapping mode. The tips used were obtained from Digital Instruments, Inc. with a force constant of 0.12 N/m. The samples were scanned at approximately 1 Hz on a 100 μ piezoelectric scanner. The scan sizes and other experimental details are provided in the figure captions.

Electrochemistry. A CHI 910B bipotentiostat (CH Instruments, Austin, TX) and a three-electrode cell were used for the electrochemical film preparation and characterization. A Ag/AgCl reference electrode and a platinum wire counter electrode were employed throughout the experiment. Throughout the experiment, all the tested solutions were bubbled with argon for at least 25 min to remove oxygen.

Results and Discussion

Film Assembly. We found that the initial electrode cleanness and overall surface charge is crucial for the successful formation of robust protein/POM LbL multilayers. After pretreatment, the glassy carbon electrode was coated with a $Ru(bpy)_3^{2+}$ layer so that the electrode surface became positively charged and thus electrostatically attractive to POMs. From there, multiple protein/POM layers could be built by either static dipping or electrochemical scanning in the appropriate adsorbate-containing solutions. In the case of static dipping, a 15 min immersion was found to be sufficient to achieve nearly complete monolayer coverage on the electrode (see below). On the other hand, we found that electrochemical cycling could produce LbL films routinely (S1, Supporting Information), but the amounts of protein and POM immobilized often varied from run to run. While in the following we focus our discussion on $P_2W_{18}O_{62}^{6-}/cyt\ c$ films formed on glassy carbon, we have had similar success in preparing LbL films using different proteins and POMs (S2 and S3, Supporting Information) and using substrates such as gold (S4, Supporting Information) and mica (see below).

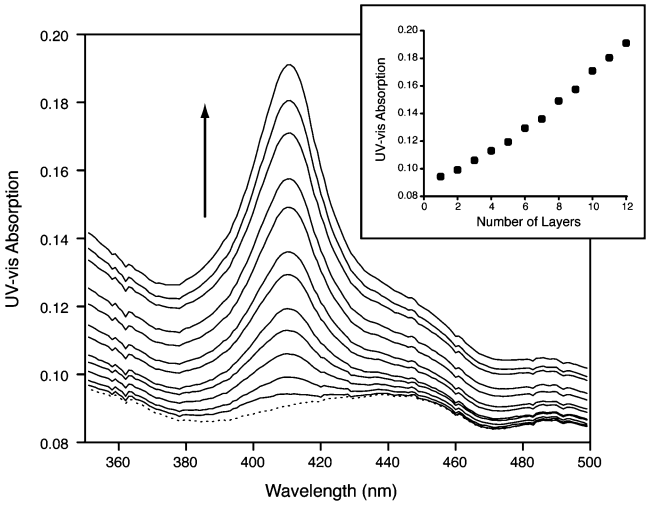

Figure 3. UV−vis absorption spectra of $\{P_2W_{18}O_{62}^{6-}/cyt\ c\}_n$ ultrathin film layer-by-layer assembled on a glass slide: dotted line, blank; solid lines show stepwise growth of $\{P_2W_{18}O_{62}^{6-}/cyt\ c\}_n$ on both sides of the glass slide, $n = 1-12$; the arrow indicates the film growth direction. Inset: layer-by-layer growth of *cyt c* absorption at 409 nm.

Characterization of LbL Films. The growth of {POM/protein}$_n$ films on glassy carbon electrodes was monitored using cyclic voltammetry in 0.1 M H_2SO_4 solution, since, as expected for Wells−Dawson anions, the POM modified electrodes only showed well-behaved, reversible redox waves under acidic aqueous conditions.[37] Representative cyclic voltammograms of $\{P_2W_{18}O_{62}^{6-}/cyt\ c\}_n$ films are shown in Figure 1a. Three pairs of reversible redox peaks with $E_{1/2}$ values at about 0 V (A/A′), −0.20 V (B_1/B_1'), and −0.43 V (B_2/B_2'), respectively, are observed between −0.5 V and +0.2 V. In addition, the peak current associated with each of the three waves increases linearly as the number of deposited layers increases.

To assign the electrochemical processes associated with each voltammetric wave, a blank film was prepared in which *cyt c* was replaced with $Ru(bpy)_3^{2+}$ (as before, $P_2W_{18}O_{62}^{6-}$ was the counterion). Because $Ru(bpy)_3^{2+}$ does not undergo electrochemical reactions in the potential region used for these measurements, all of the redox features observed from the blank film could be assigned to the POM. As shown in Figure 1b, two pairs of reversible waves are seen (B_1/B_1' and B_2/B_2'). The reductive voltammetry of the Wells−Dawson POMs series in acidic aqueous media is well studied; typically, four reversible waves between 0 V and −0.75 V are observed. The first two

(36) Zhan, W.; Alvarez, J.; Crooks, R. M. *J. Am. Chem. Soc.* **2002**, *124*, 13265−13270.

(37) Xi, X. D.; Dong, S. J. *J. Mol. Catal. A: Chem.* **1996**, *114*, 257−265.

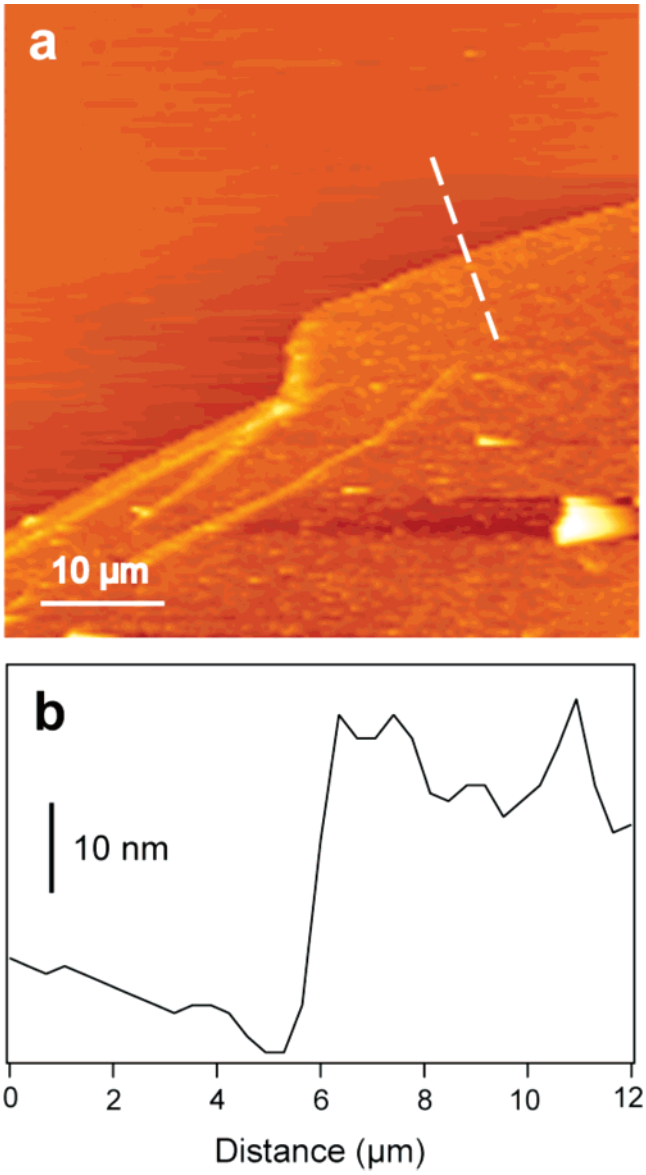

Figure 4. Determination of LbL film thickness using AFM. (a) Tapping mode AFM imaging was used to profile lithographically defined patterns in LbL films. An area of the patterned film containing regions of bare mica as well as a $\{P_2W_{18}O_{62}^{6-}/cyt\ c\}_{10}$ film is shown. (b) The height profile as measured along the dashed line in the image a.

waves are one-electron reductions and the second two waves are two-electron/two-proton reductions. In the case of both the $\{P_2W_{18}O_{62}^{6-}/cyt\ c\}_n$ and $\{P_2W_{18}O_{62}^{6-}/Ru(bpy)_3^{2+}\}_n$ films studied here, it appears that the first wave (B_1) is a two-electron wave. This behavior has been reported before, at extremely low pH values, in the case of transition metal substituted Wells−Dawson compounds and in $P_2W_{18}O_{62}^{6-}$/poly(1-naphthol) films.[38] Based on these considerations, the electrochemical processes associated with peaks B_1/B_1' and B_2/B_2' can be described by the following reactions:[23]

$$P_2W_{18}O_{62}^{6-} + 2e^- = P_2W_{18}O_{62}^{8-} \quad (1)$$

$$P_2W_{18}O_{62}^{8-} + 2H^+ + 2e^- = H_2P_2W_{18}O_{62}^{8-} \quad (2)$$

The amount of $P_2W_{18}O_{62}^{6-}$ immobilized in each layer was calculated from the integrated charges of wave B_2 or B_2' to be

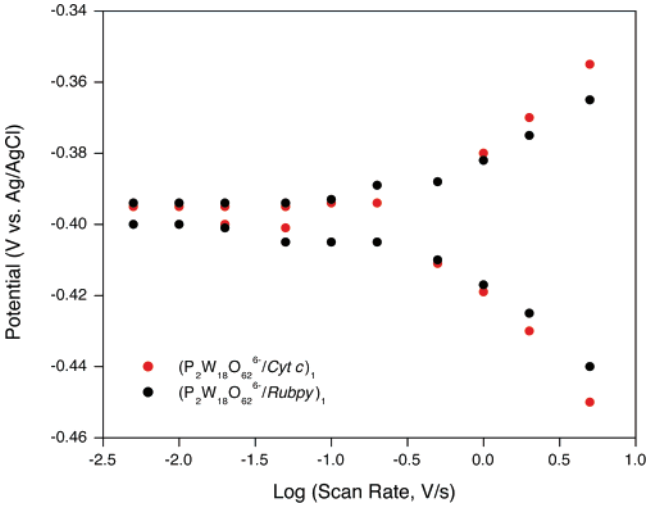

Figure 5. Determination of the apparent electron-transfer rate constants (k°_{app}) for $\{P_2W_{18}O_{62}^{6-}/cyt\ c\}_1$ and $\{P_2W_{18}O_{62}^{6-}/Rubpy\}_1$ films following Laviron's method.[44] Peak potentials were collected from the CVs at different scan rates in degassed 0.1 M H_2SO_4 aqueous solutions.

Table 1. Change of k°_{app} (s^{-1}) as a Function of the Number of LbL Layers

n	$(POM/Rubpy)_n$	$(POM/cyt\ c)_n$
1	31.7	26.4
2	20.0	19.8
5	10.6	4.0

$1.5-1.6 \times 10^{-10}$ mol/cm^2, which corresponds to a nearly full monolayer coverage.[21]

Figure 1c is an overlay of CVs obtained from $\{P_2W_{18}O_{62}^{6-}/cyt\ c\}_2$ and $\{P_2W_{18}O_{62}^{6-}/Ru(bpy)_3^{2+}\}_4$ films. On the basis of this data, we assign the couple (A/A′) around 0 V to the direct reduction (oxidation) of *cyt c*. It should be noted that the formal potential of *cyt c* in the $\{P_2W_{18}O_{62}^{6-}/cyt\ c\}_2$ film is shifted to more negative values than what is typically observed for *cyt c* in solution or in uncharged monolayer films.[39] The interaction of *cyt c* with the negatively charged POM would be expected to stabilize the oxidized form of the protein and cause $E_{1/2}$ to shift to more negative values, consistent with our observations. Similarly, the $E_{1/2}$ values of the POM wave (B_1) shifts to more positive potentials, as the interaction of anionic POMs with positively charged regions on the surface of the protein is expected to stabilize the reduced form of the POM. Also evident in the $\{P_2W_{18}O_{62}^{6-}/cyt\ c\}_n$ films is that the peak splitting becomes greater as the number of layers increases, which could arise from a modified electronic microenvironment as a result of the interaction between $P_2W_{18}O_{62}^{6-}$ and *cyt c*. Nevertheless, the integrated charges of wave $B_1(B_1')$ remain comparable between the two films, indicating that the additional peaks (A(A′)) are indeed due to *cyt c* redox processes.

Voltammetric measurements carried out on $\{P_2W_{18}O_{62}^{6-}/Ru(bpy)_3^{2+}\}_n$ films at different scan rates reveal that the POM peak currents are proportional to the scan rate up to 0.5 V/s at $n = 8$, consistent with the electrochemical behavior expected from a surface-confined species.[40] In contrast, the scan rate dependence we observed in the case of $\{P_2W_{18}O_{62}^{6-}/cyt\ c\}_n$ films appears more complex. Figure 2a shows how the normalized peak current of B_2' changes with the number of $P_2W_{18}O_{62}^{6-}/cyt\ c$ multilayers at different scan rates. For the four different scan rates tested

(38) Pham, M. C.; Moslih, J.; Chauveau, F.; Lacaze, P. C. *J. Appl. Electrochem.* **1991**, *21*, 902−909.

(39) Liu, H. Q.; Tian, Y.; Deng, Z. F. *Langmuir* **2007**, *23*, 9487−9494.

(40) Bard A. J.; Faulkner L. R. *Electrochemical Methods-Fundamentals and Applications*, 2nd ed.; John Wiley & Sons, Inc: New York, 2001.

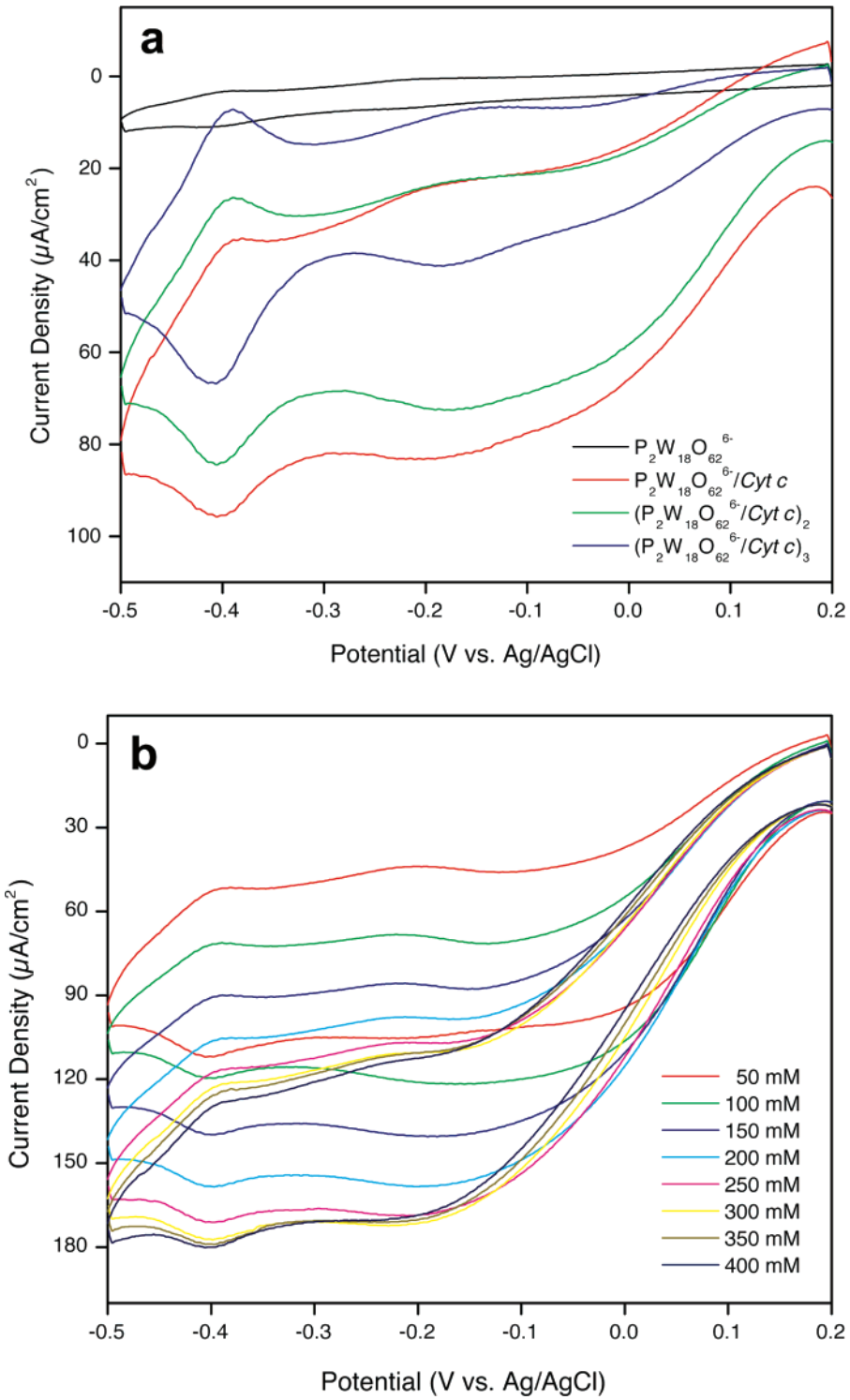

Figure 6. Electrocatalysis of hydrogen peroxide reduction using $\{P_2W_{18}O_{62}^{6-}/cyt\ c\}_n$ films. (a) Dependence of catalysis efficiency on film thickness. $\{P_2W_{18}O_{62}^{6-}/cyt\ c\}_n$ ($n = 1-3$) films were examined using 50 mM H_2O_2; supporting electrolyte, 0.1 M KCl in 0.1 M phosphate buffer (PBS), pH = 7.3. (b) Catalysis of hydrogen peroxide reduction using $\{P_2W_{18}O_{62}^{6-}/cyt\ c\}_n$ ($n = 1$) modified GCEs at different H_2O_2 concentrations; other conditions are the same as in (a).

(0.5, 0.1, 0.02, and 0.005 V/s), the maximum peak current occurs at layer numbers of $n = 3$, 5, 9, and 12, respectively. At relatively high scan rates, the peak currents first decrease beyond the maximum and then level off, suggesting that the scan rate has exceeded the rate of electron transfer through the multilayer.[15] If this is true, then measurements at low scan rates should approach the ideal linear dependence of peak current on scan rate. Indeed, when the scan rate is lowered to 0.005 V/s, all 12 layers are electrochemically accessible (Figure 2b). More quantitative measurements on charge transport through these films will be discussed in the next section.

UV−vis absorption spectroscopy was also used to characterize the formation of $\{P_2W_{18}O_{62}^{6-}/cyt\ c\}_n$ films, since *cyt c* has an intense Soret band at around 409 nm (Figure 3). The increase in absorption at 409 nm was found to be directly proportional to the number of layers deposited and is consistent with our cyclic voltammetry results. Moreover, the well-defined band shapes of the UV−vis spectra suggest that the tertiary structure

of *cyt c* has not been significantly perturbed during the LbL assembly process. From the increase in absorption, the average coverage of *cyt c* in each layer is calculated to be close to one monolayer, that is, $\sim 2.2 \times 10^{-11}$ mol/cm^2.[41−43] The inset to Figure 3 shows a plot of absorption peak intensity as a function of layer number. Interestingly, there is a small but noticeable increase in the slope of this graph after about the fifth layer. Similar behavior has been observed in the case of polymer-based LbL films.[31]

AFM Characterization of $\{P_2W_{18}O_{62}^{6-}/cyt\ c\}_n$ Films. Owing to the intrinsic negative surface charge, mica surfaces are ideal for forming POM/*cyt c* LbL films. Combining LbL assembly and a previously published microfabrication technique,[36] we were able to fabricate simple patterned LbL films and measure the film thickness directly using atomic force microscopy to profile lithographically defined step edges. A typical AFM image of $\{P_2W_{18}O_{62}^{6-}/cyt\ c\}_{10}$ film near one such step edge is shown in Figure 4. The upper left portion of the image shows an exposed region of the bare mica substrate, while the more textured region in the lower part of the image reveals the topography of the LbL film. The linear features that can be seen near the step edge are film defects and do not correspond to individual monolayer steps. In this image, a step height of ∼40 nm was obtained when the tip was scanned from the mica substrate to the patterned film. This result is in good agreement with the physical dimensions of the POM (∼1 nm) and the protein ($\sim 3 \times 3 \times 4$ nm) used as well as the number of film layers prepared.

Effect of Film Thickness on Overall Electron-Transfer Rate. Following Laviron's approach,[44] we examined the effect of LbL film thickness on the electron-transfer rate by studying the redox peak splitting as a function of the scan rate. For this purpose, we chose the second reduction/oxidation peak of $P_2W_{18}O_{62}^{6-}$ (B_2/B_2') because it is well resolved in cyclic voltammetry. In this analysis, cathodic and anodic peak potentials are plotted as a function of the logarithm of the scan rate, and the limiting slope of the resulting plots at high scan rate is used to determine the apparent electron-transfer rate constant, k°_{app}. Typical Laviron plots are shown in Figure 5 for $\{P_2W_{18}O_{62}^{6-}/cyt\ c\}_1$ and $\{P_2W_{18}O_{62}^{6-}/\text{Rubpy}\}_1$ films. Table 1 shows in addition the $P_2W_{18}O_{62}^{6-}$ rate constant for films of different thickness assuming $\alpha = 0.5$. Clearly, the electron transfer slows down as the film becomes thicker in both preparations; in particular, the rate decrease is faster for $\{P_2W_{18}O_{62}^{6-}/cyt\ c\}_n$ films as a result of the larger building block (*cyt c* vs $Ru(bpy)_3^{2+}$) and thus thicker films.

Electrocatalysis of Hydrogen Peroxide Reduction Using $\{P_2W_{18}O_{62}^{6-}/cyt\ c\}_n$ Films. An important application of electroactive LbL films is their electrocatalysis, as hybrid films prepared in this manner can dramatically enhance the reduction/oxidation of many species that otherwise only display sluggish electrochemical behavior. We chose to test the electrocatalytic reduction of hydrogen peroxide using our films because *cyt c* is known to be catalytically active for H_2O_2 reduction.[45,46] As shown in Figure 6a, the film containing both $P_2W_{18}O_{62}^{6-}$ and *cyt c* enhances the electroreduction of H_2O_2 by greater than 10-fold as compared to that from a film having $P_2W_{18}O_{62}^{6-}$ only. In addition, if $\{P_2W_{18}O_{62}^{6-}/cyt\ c\}_n$ films are used, the reduction current actually decreases as the number of layers increases. These results indicate that the catalytic activity of the films is dominated by the contribution of *cyt c*. Using films containing a single layer of $P_2W_{18}O_{62}^{6-}$ and *cyt c*, we found that the reduction current of H_2O_2 increases nearly linearly up to 250 mM and then levels off, suggesting the catalysis follows a typical Michaelis−Menten behavior.[47]

Conclusions

It was with two questions in mind that we set out to prepare POM/protein thin films using electrostatic LbL assembly. First, is it possible to use highly charged inorganic species such as POMs and macromolecules such as proteins to replace conventional polyelectrolytes in forming such assemblies? Many nanoscopic building blocks have been incorporated into LbL films. However, polymeric polyelectrolytes are almost always used as the counterparts in such films. In this regard, we have clearly demonstrated that polyoxometalates represent suitable materials, owing to their extremely small size, intrinsic charges, and chemical stability. In fact, electrochemical and UV−vis absorption spectroscopic characterization confirm a nearly monolayer-by-monolayer growth of POMs and proteins when they are deposited by static dipping. Second, we were also curious to know if films formed using these unconventional building blocks can facilitate direct electrochemistry of redox proteins when the latter are assembled. The experiments we have done so far indicate that secondary structural considerations such as POM/protein complex formation and protein orientation may play an important role in the observed electron-transfer kinetics and catalyst performance. While $\{P_2W_{18}O_{62}^{6-}/cyt\ c\}_n$ films formed by our method clearly show enhanced reduction of hydrogen peroxide, the catalytic efficiency is somewhat lower, for example, than in the case where negative-charge-terminated gold nanoparticles are used to assemble *cyt c*. This result from another perspective emphasizes that many, sometimes subtle, requirements need to be met experimentally before a strong electrochemical communication can be established between redox proteins and the electrodes. Can we design new POM structures to better accommodate redox proteins in LbL assembly? Is it possible to induce a higher level of control of the protein orientation on electrode using POMs? These are the questions we hope to find answers to in the near future. Recent studies of POM/protein interactions that show well-defined binding sites and stoichiometries with no denaturation are quite promising in this regard.[48]

Acknowledgment. Financial support for this work was provided through new faculty start up funds and the Auburn University Faculty Mentoring Grant Program. We thank Anand Sankarraj and Chaokang Gu for technical assistance and helpful discussions.

Supporting Information Available: POM−protein LbL formed through multiple electrochemical scans, LbL formation using different proteins and POMs and using gold substrate. This material is available free of charge via the Internet at http://pubs.acs.org.

LA704015J

(41) Kimizuka, N.; Tanaka, M.; Kunitake, T. *Chem. Lett.* **1999**, 1333−1334.
(42) Wood, L. L.; Cheng, S. S.; Edmiston, P. L.; Saavedra, S. S. *J. Am. Chem. Soc.* **1997**, *119*, 571−576.
(43) The thin film of $P_2W_{18}O_{62}^{6-}$ and *cyt c* is formed on both sides of the glass slide. The average increase in absorbance at 409 nm is about 4.18×10^{-3} for each bilayer of $P_2W_{18}O_{62}^{6-}$ and *cyt c*, and this value is very close to that estimated for a closely packed monolayer of *cyt c* (4.2×10^{-3}).
(44) Laviron, E. *J. Electroanal. Chem.* **1979**, *101*, 19−28.
(45) Wang, J. X.; Li, M. X.; Shi, Z. J.; Li, N. Q.; Gu, Z. N. *Anal. Chem.* **2002**, *74*, 1993−1997.
(46) Zhao, G. C.; Yin, Z. Z.; Zhang, L.; Wei, X. W. *Electrochem. Commun.* **2005**, *7*, 256−260.
(47) Kamin, R. A.; Wilson, G. S. *Anal. Chem.* **1980**, *52*, 1198−1205.
(48) Zhang, G.; Keita, B.; Craescu, C. T.; Miron, S.; de Oliveira, P.; Nadjo, L. *J. Phys. Chem. B* **2007**, *111*, 11253−11259.